*Near Surface Geophysics, 2009,* 227-236

# Hydrocarbon contaminated soil: geophysical-chemical methods for designing remediation strategies

Daniel Coria[1], Victoria Bongiovanni[2,3,4*], Néstor Bonomo[2,3], Matías de la Vega[2,3] and María Teresa Garea[4]

[1] *Facultad de Ciencias Empresariales, Universidad Abierta Interamericana, Av. Pellegrini 1957, Rosario, Santa Fe, Argentina*
[2] *Grupo de Geofísica Aplicada y Ambiental, Departamento de Física, Facultad de Ciencias Exactas y Naturales, Universidad de Buenos Aires, Ciudad Universitaria, Pabellón 1, 1428 Buenos Aires, Argentina*
[3] *CONICET, Consejo Nacional de Investigaciones Científicas y Técnicas (National Council of Scientific and Technical Investigations), Avda. Rivadavia 1917, CP C1033AAJ, Ciudad de Buenos Aires, Argentina*
[4] *Facultad de Ingeniería, Universidad Austral, Avda. Juan de Garay 125, C1063ABB, Ciudad de Buenos Aires, Argentina*

Received October 2007, revision accepted April 2009

**ABSTRACT**

Rapid and correct characterizations of contaminant plumes are necessary to plan efficient and economically viable remediations of affected zones. In this context, we have carried out a joint implementation of two geophysical non-invasive methods and chemical monitoring from wells to characterize an area affected by a hydrocarbon spill caused by a traffic accident involving a transport truck and its trailer. The studied area is situated in Alejo Ledesma, Argentina and has an area of 4350 m$^2$. The geophysical prospecting was carried out through the resistivity and the electromagnetic induction methods. The first method provided precise vertical resistivity sections, which were acquired at representative contaminated/uncontaminated sectors, whereas the second allowed a quick prospecting of the entire area. The chemical procedure consisted of samples obtained from a small number of monitoring wells, which were located at selected positions. We correlated the geophysical interpretations with the chemical data to delimit the zone affected by the spill. The detection and characterization of the contaminated plume by the geophysical methods showed positive results even though a liquid phase was not present at the site. A remediation methodology could be determined from these results. The efficiency of the applied methodology (stabilization/solidification) was also confirmed through these methods.

## INTRODUCTION

A priority of groundwater management is the protection of water quality in aquifers. There are many artificial sources of potential groundwater contamination and one of the most important is due to hydrocarbon exploitation and transportation. Frequent accidents happen during transportation of different hydrocarbon products along pipelines and trucks, or from buried storage tanks in gas stations, refineries and industrial plants. These events produce leaking of the hydrocarbon directly on the ground. Reliable strategies should be developed to prevent further spreading of these contaminants and the possible degradation of water quality.

Remediation efficiency and costs depend basically on a precise and quick diagnosis of the spill. Once a spill occurs, a number of items should be addressed before the site remediation method can be selected and applied. The first item is to locate the source of the contamination. Second, it is necessary to know how contaminants extend and propagate in the subsurface, which are a function of the hydrogeological characteristics of the surrounding media. This information is then used to evaluate the probability of the contaminant reaching an aquifer, or flowing from one aquifer to other. An answer to each of these aspects is required to determine the adequate methods for soil and aquifer remediation.

One way to characterize a contaminated area is by determining the electrical resistivity distribution of the affected zone and its surroundings. If the contaminated soil and unpolluted soil have different electrical properties, the contaminant plume can be distinguished as an electrical anomaly. Usually, hydrocarbon spills produce resistive anomalies immediately after the spill but after several months the resistivity diminishes due to the contaminant biodegradation (Sauck *et al.* 1998; Atekwana *et al.* 2000; Sauck 2000; Abdel *et al.* 2004). However, under particular conditions this effect could be absent (de la Vega *et al.* 2003). Then, a central point in the physical-chemical investigations is to

* bonvik@df.uba.ar

properly determine the resistivity levels of the contaminated portions of the soil. For example, Shevnin *et al.* (2006) compared geoelectric data to a petrophysical theoretical model to interpret the resistivity distribution at a mature spill. An alternative way to interpret the electrical profiles is to identify the resistivity of the contaminated zones with the resistivity obtained from geoelectric soundings performed at the same locations where chemical analyses of wells indicate high contamination levels (see e.g., Osella *et al.* 2002; Frohlich *et al.* 2008).

In the present work we jointly use the electromagnetic induction (EMI) method, the geoelectrical method and chemical sampling from wells, for a rapid localization of a hydrocarbon plume in a zone where a tanker overturned at a side of a road. The EMI method allowed a fast prospecting of the entire zone, whereas the geoelectrical method provided accurate vertical profiles at a number of relevant positions. The electric anomalies due to contamination were identified through the comparison of the geophysical and chemical results. The joint implementation allowed an effective delineation of the affected portions of soil and results were obtained faster than previous studies (Osella *et al.* 2002), without a decrease in precision. Based on the joint geophysical information, a remediation methodology was more efficiently selected and applied. Finally, these methods were also used to monitor the zone after the remediation to determine the efficacy of the remediation strategy.

## GEOPHYSICAL METHODS

The first objective of this work was to obtain an electrical map of the subsurface, so as to precisely delimit the contaminated zones, prior to the remediation of the site. In this work we jointly used two different geophysical methods, the EMI and the geoelectrical method. The first has the advantage of allowing a rapid prospecting of extended areas, whereas the second often provides more accurate resistivity profiles, thus they complement each other. The joint implementation also enhances the resolution of the prospecting, since each method presents different sensitivity and resolution according to the physical properties of the different materials.

### Electromagnetic surveys

Electromagnetic methods allow mapping the electrical resistivity of the ground. In particular, the methods that use small-loop frequency-domain systems are especially adequate for environmental problems (Reynolds 1997). One of the main advantages of these systems is that the acquisition process does not require direct contact with the ground, as in the case of other electromagnetic methods and consequently, they are much quicker. This kind of system consists of two small coils, a transmitter and a receiver separated by a constant distance, which are moved along a trajectory. The secondary field detected at the receiver is separated into in-phase ($H_I$) and quadrature ($H_Q$) components, which are expressed in ppm (parts per million) against the primary field produced by the transmitter. The in-phase component depends both on the magnetic permeability and the conductivity (the inverse of resistivity) of the soil and is usually noisier than the other component. The quadrature component is related to the distribution of electrical conductivity (more precisely, the apparent conductivity) as a function of the frequency *Freq*, through the expression (Won *et al.* 1996):

$$\sigma_a = 0.360 * \frac{H_Q(ppm)}{Freq(S/m)} \quad (1)$$

Due to the range of frequencies involved, the process is purely diffusive. The penetration is governed by the skin-depth

$$\delta = \sqrt{\frac{2}{\varpi\sigma\mu}} \quad (2)$$

where $\omega$ is the angular frequency ($2\pi Freq$), $\sigma$ the conductivity of the medium and μ the magnetic permeability.

In this work we used the Geophex GEM-2 equipment (based on the work of Won *et al.* 1996). It has a frequency range from 330–47970 Hz, allowing a maximum of 15 simultaneous survey frequencies, though usually 6 frequencies were used, guaranteeing good signal-to-noise quotient. We performed in-line surveys (axis between the two coils coincident with the direction of survey lines), with the coil axis perpendicular to the ground. Each sector was covered with parallel lines with 1m-separation, in two orthogonal directions and data were collected with a step of 0.05 m. The data collected along each profile were inverted using a 1D inversion code, EM1D v1.0 (Farquharson *et al.* 2000). An analysis of each profile was done to remove possible outliers that could distort the inversion procedures. Pseudo-3D resistivity images were constructed from 1D results. The electrical images obtained from this methodology often give accurate descriptions of the subsurface resistivity (Bongiovanni *et al.* 2008).

### Geoelectrical surveys

In the geoelectrical method, a constant electrical current is injected into the ground through two electrodes and the potential difference is measured at another two points through another pair of electrodes. The quotient between voltage and current, multiplied by a geometrical factor that depends on the electrode configuration, defines an apparent resistivity (in ohm.m), which contains the information about the distribution of the electrical resistivity of the subsoil. Then, data are inverted in order to obtain the true electrical distribution of the soil. As in the case of the electromagnetic surveys, buried structures can be detected as contrasts or anomalies in the electrical properties of the medium.

As this study required high lateral resolution but shallow penetration we used dipole-dipole arrays with electrode separation of 0.5 m and 1m and maximum dipole separation factor n = 6. Data were collected using the multielectrode resistivimeter Saris 500 (www.scintrexltd.com). To invert the data we used the DCIP2D inversion code developed by the University of British Columbia (2000) and based on the works of Oldenburg and Li (1994) and Oldenburg *et al*. (1993). The quality of the inversion

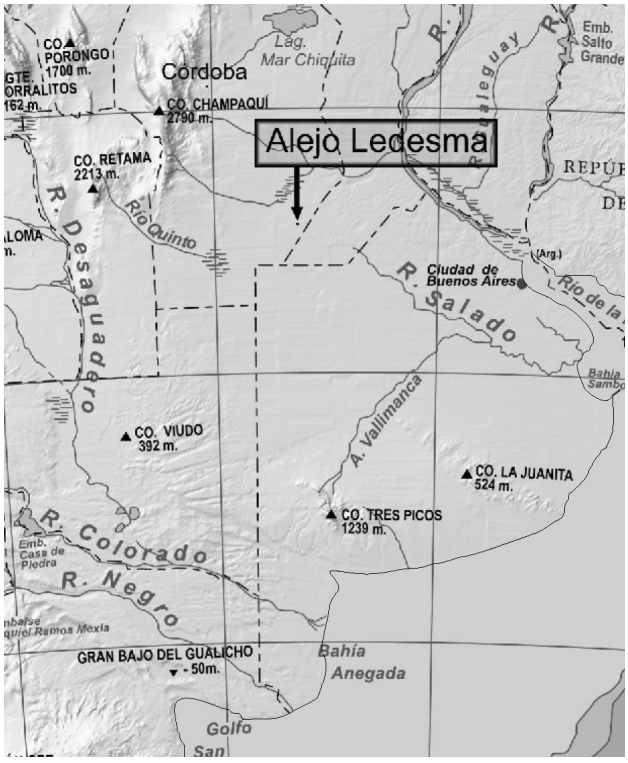


FIGURE 1
Location of Alejo Ledesma, where the accident occurred.

TABLE 1
Chronological summary of the main events

| | |
|---|---|
| August 2003 | The tanker overturns |
| December 2004 | First series of chemical analyses |
| March 2006 | First geophysical survey |
| August 2006 | Second series of chemical analyses |
| August 2006 | Remediation |
| October 2006 | Second geophysical survey |

process was verified by the misfit, i.e., the distribution of the difference between the observed and predicted data, normalized by the standard deviation. A measure of the quality of the inversion process is given by this parameter.

## SITE DESCRIPTION

The accidental hydrocarbon spill took place when a tanker overturned at the south verge of National Road, 8.3 km away from Alejo Ledesma town, Córdoba Province, Argentina, on 31 August 2003 (see Fig. 1). The spilled quantities were 9 000 litres of gasoline and 27 000 litres of diesel. The area that was directly affected by the leakage approximately extends 700 m$^2$, as determined by the first *in situ* inspections. Due to legal matters, geophysical studies started three years later.

A chronological summary of the main events at the site is shown in Table 1 and a scheme of the prospected area is shown in Fig. 2. The different surveys and the monitoring wells we performed are indicated in this figure. The liquid of the truck was spilled at point P2 (see Fig. 2), whereas the liquid of the trailer between P6 and P7, approximately, though nearer P6. There was a soy cultivation on the other side of the wire fence (which is represented by a dashed line in Fig. 2). Parallel to the road and 20 m from the origin of coordinates, there existed a line of trees, which were spread approximately every 12 m.

### Lithological description

The studied area is located in the geomorphological environment that predominates in the north-east of Buenos Aires Province, known as Pampa Ondulada and in particular in the Llanura Pampeana Alta. The calcareous loessoides silt of the upper Pampeano formation is formed from sandy and clayey silt with varying amounts of calcareous material. Beneath the Pampeano formation is the Arenas Puelches formation, a stratum of clean yellowish quartz sand with a variable percentage of mica and ferric oxide. The Arenas Puelches formation shows a particle size reduction from the bottom to the top, changing from coarse-grained sand to medium and fine-grained sand. The lower formation within the study area is the Paraná formation, which has a

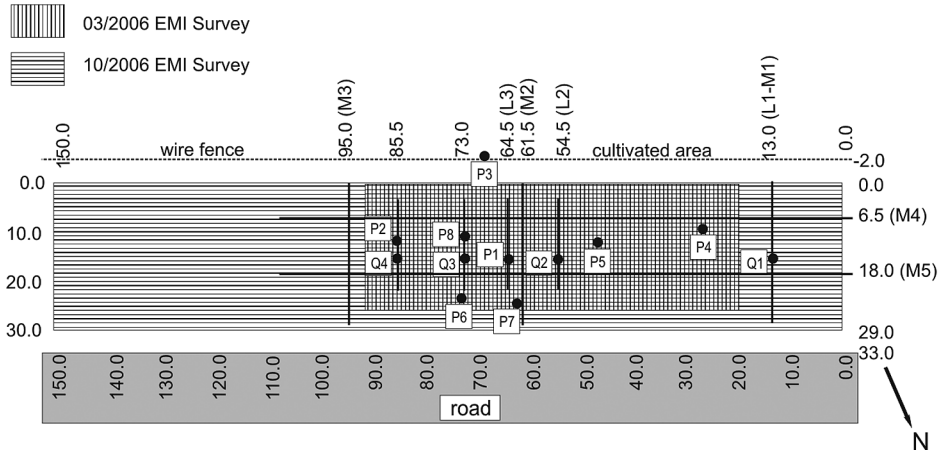


FIGURE 2
Surveyed areas. The vertical and horizontal grey patterns respectively indicate the EMI prospected zones, before and after the remediation. Dipole-dipole geoelectric lines that were acquired before (L#) and after (M#) the remediation are marked through dark lines. Monitoring wells that were drilled immediately after the accident (P#) and some days before remediation (Q#) are indicated through dots.

marine origin and is formed by green or green-blue clay. The Paraná formation, at a depth of 70 m below ground surface, is the basis of the Puelche aquifer.

The lithological profile obtained from wells drilled at the accident zone showed that the subsoil is mainly composed of fine-grained, silted sand up to a depth of 5 m (this corresponds to the Arenas Puelches formation). The water table is at least at 2.5 m depth, depending on topography. Towards the west, a gradient of 0.002 in the topography was observed on the surface. The lowest levels in the NS direction occurred between 7–12 m, along a fringe parallel to the road, with greater gradients near to this road and to the wire fence.

## DATA ACQUISITION AND ANALYSES

### Before remediation

*First chemical analyses*

The first chemical analyses were made 16 months after the accident by means of eight monitoring wells (P1–P8 in Fig. 2); all of them, except P3, distributed throughout a surface without vegetation, which corresponds to the area apparently affected by the fuel. Samples of the strata were obtained up to a depth 3 m under the surface level. These samples were used both to carry out the descriptions of the lithological profiles and to perform laboratory chemical analyses. Phreatic water was also extracted from the same wells from a depth of isolation between 4.5–5.5 m under the surface level. No presence of NAPL (Non-Aqueous Phase Liquid) was detected in any of the eight monitoring wells installed in the area neither during the perforations, nor during the six-month interval monitoring performed after them.

The results of the analysis of PTH (Polinuclear Total Hydrocarbons) are shown in Table 2 (EPA 418.1) and refer to contaminant per dry kg of soil. The limit of detection of the method is 0.5 mg. For example, the result for P3, 51.4 mg/kg, allowed us to know the amount of hydrocarbon in the soil, because it was drilled far from the most contaminated zone. On the other hand, 1000 mg/kg is the maximum amount of hydrocarbon allowed in Argentina. Then, P2, P5, P6 and P8 presented concentrations above the legal limit. Fortunately, in these cases the analyses of water samples from the phreatic zone showed concentrations of dissolved hydrocarbons clearly below the allowed limit by Argentinean legislation.

From the soil sample results we observe that the contaminant distribution is not homogeneous. For example, at 1 m depth, the maximum pollution is observed in P6, whereas at 2 m depth it is observed in P8 and P2. For a depth of 3 m the contaminant level decreases abruptly (only traces in the phreatic zone were detected). We also notice that although the monitoring well P1 is located near to P6 and P7, in P1 the level of contaminant is very low in relation to them. On the basis of this information, we see that the contaminated plume at least extended from 46.5 m (P5) to 85.5 m (P2) parallel to the road and from 29–6.5 m perpendicular to the road (see Fig. 2).

TABLE 2

First series of analyses of Polinuclear Total Hydrocarbon (PTH), Environmental Protection Agency (EPA) 418.1

| Depth (m) | P1 (mg/kg) | P2 (mg/kg) | P3 (mg/kg) | P4 (mg/kg) | P5 (mg/kg) | P6 (mg/kg) | P7 (mg/kg) | P8 (mg/kg) |
|---|---|---|---|---|---|---|---|---|
| 1 | 542.7 | 2371.4 | | 495.3 | 1912.4 | 15,906.4 | 1862.1 | 1153.6 |
| 2 | 500.8 | 1907.0 | | 529.4 | 642.7 | 867.9 | 564.8 | 2813.6 |
| 3 | 371.0 | | 51.4 | | | | 231.8 | 400.4 |

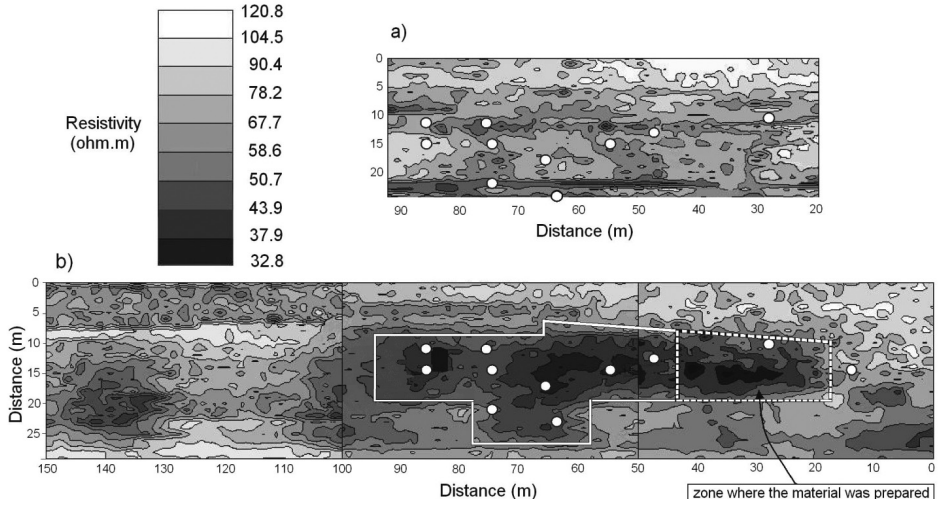


FIGURE 3

Slice of the inverted EMI data, for a depth 1 m. a) Data acquired before remediation and b) after remediation. The white circles indicate the well locations (see Fig. 2 for the labelling). The white solid lines show the limits of the remediated area and the dashed lines the zone where the materials were prepared.

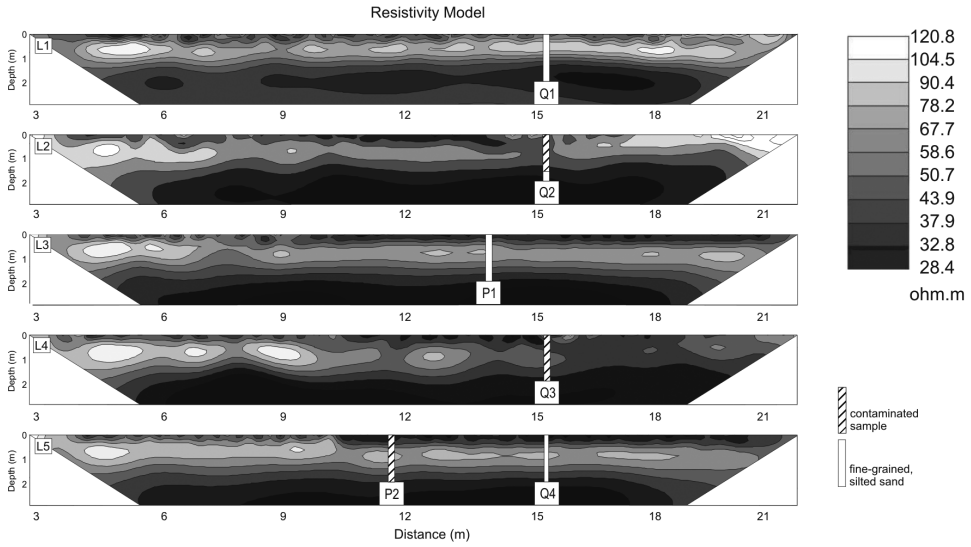


FIGURE 4
Resistivity profiles before remediation. The first and second series of monitoring wells are indicated with P# and Q#, respectively. We shaded those parts of the wells in which contaminated samples were obtained.

*Geophysical survey with EMI*

In March 2006, we covered the entire sector with EMI profiles for a fast localization of the anomalous zones. The surveyed area is shown in Fig. 2. Once the data were acquired, we inverted them to obtain electrical images of the subsoil. For example, Fig. 3(a) shows a slice at 1 m depth. White circles indicate the location of the monitoring wells (see also Fig. 2).

As a first interpretation of the EMI data, we correlate them to the chemical analyses and the lithological information. In the next sections we will correlate these results to the geoelectrical ones. Because of the homogeneity observed up to 3 m in almost all the sector, except for the fringe near the road, we can *a priori* attribute the different electrical behaviours to different contamination and/or moisture levels. P1 and P4, which had a low level of hydrocarbon concentrations according to the chemical results (Table 2), present in Fig. 3(a) more resistive zones (70 ohm.m) than their surroundings. P6 and P7, which were contaminated, have lower resistivity values, around 40 ohm.m. However, in these cases such low values could be due to the fact that these areas are located near the road, where the soil presents a mixture of natural soil, sand and construction materials that could further decrease the resistivity (besides the effect of the contaminant). In P5 and P8, which are located far from the road and where contamination was obtained, the resistivity values are between 50.7–58.6 ohm.m. We also note in Fig. 3(a) two zones with resistivities in this range, approximately located around the positions 75 m and 50 m and extending perpendicularly to the road, which can be *a priori* considered as affected zones. Finally, although the chemical analyses presented contamination at P2, the resulting resistivity was larger than 58.6 ohm.m and similar to the values of unaffected zones. We will see later that this result is also obtained from the geoelectric data.

*Geophysical survey with resistivity method*

Simultaneously, dipole-dipole profiles, indicated with L# in Fig. 2, were performed in the zone in which well data showed the largest amounts of contaminant, except for L1 that was located outside this area. On the basis of the results from this profile we could analyse the other ones, since we had no pre-spilled data.

We inverted the data using the DCIP2D inversion code. Control parameters required by the program were selected to reach a good convergence. We achieved standard deviation values less than 10% for all the profiles.

Figure 4 shows the inversion results obtained from the surveys that were performed perpendicular to the road. The monitoring wells that coincided with these lines are also indicated in the figure (P1 and P2).

Up to a depth approximately 1 m in L1 we observe a homogeneous resistive layer of about 100 ohm.m. In this zone, far from the accident point, monitoring well P1 and EMI data had proved no signs of contamination above the legal limit. In profile L2, which was situated between P5 and P7 and where pollutant was registered, we observe a similar resistive layer, although in this case the layer presents a lower resistivity discontinuity between 9–17 m. Note that the extension and resistivity of this anomalous zone (about 50 ohm.m) agree with the EMI results.

Figure 4 also shows that L4 presents similar characteristics to L2; the anomalous zone is very evident from 10–21 m. We also observe that this anomaly is more important towards the end of the line, where the chemical analyses revealed a maximum of contamination (see the values in P6, which was located close to this end). On the contrary, the L5 upper layer is rather homogeneous even though pollutant was originally detected in P2. In the monitoring well P1, where a small quantity of pollutant was found, it seems that hydrocarbons were not sufficient to sensitively affect the resistivity value of the layer (see profile L3 in Fig. 4). Note that all these results match up the observations performed from the EMI data.

As the chemical analyses indicated, the contaminant did not form a NAPL in this case and the solid pores were not saturated by the hydrocarbon. In spite of this, the geophysical characterization has given satisfactory results. These results suggest that

the resistivity at the contaminated zones is lower than at the uncontaminated zones, probably due to the biodegradation process and that the contaminated zone involved about 1200 $m^3$. Nevertheless, considering the contradictory results for L5 and the long period of time between the first series of chemical analyses and the geophysical measurements, four additional wells were drilled so as to check our interpretations.

*Second chemical analyses*

In August 2006, before the site remediation, a second series of wells (indicated by Q# in Fig. 2) were drilled according to the results of the geophysical studies. Four soil samples between 0.5–2.0 m depth were extracted from each well, to be analysed. Table 3 shows the results obtained for PTH (EPA 418.1) in mg per dry kg. No pollutant was found in the water analyses from the P# monitoring wells since the accident.

The Q# results confirm our interpretation of the geophysical data. There is pollutant in Q2 and Q3, at the same positions where we had detected electrical anomalies in L2 and L4 (the measured resistivities were 43.9 ohm.m and 58.6 ohm.m at these positions). Where the electrical images had not presented anomalies, no pollutant was detected; Q1 corresponds to L1 and Q4 to L5.

The altitude of the soil slightly diminishes towards the west (from P6 to P7) so we interpret that this allowed an initial flux of pollutant in the surface from P6 (where the spillage of the trailer content was) towards P7. Nevertheless, a small mound located between P7 and P6 and close to P1 seems to prevent a greater flux between them (and probably to P5). Then, most of the pollutant accumulated and infiltrated close to P6. Also because of this, in P1 and L3 neither a high level of pollution nor electrical anomalies in the upper layer occurred.

*Analysis of the relation between resistivity and contamination levels*

In this section we further analyse the relation between the measured resistivity and the pollutant concentration. To do this we consider the results from the resistivity method, which are usually more accurate than the EMI ones.

Figure 5 shows the distribution of mean resistivity versus contamination level, for Q1, Q2, Q3 and Q4. Each datum has been obtained by vertically averaging between the limits of the respective depth interval (the same limits as in the chemical characterization: 0.0–0.5 m, 0.5–1.0 m, 1.0–1.5 m, 1.5–2.0 m) and horizontally averaging around each well position (±0.5 m). The data labels in the figure indicate the respective geoelectric profile, whereas the correspondence between the geoelectric profile and the well denominations has been indicated in the lower-right box.

It can be observed in Fig. 5 that the first three shallow intervals present increasing resistivity with the concentration of contaminant. For a better visualization of the tendencies, points belonging to a same interval have been linked through a curve. Point L1 for the interval 1.0–1.5 m was not included in the respective curve since it clearly presents a lower resistivity, deviating from the general tendency, probably due to a closer proximity to the phreatic zone at this point, as the well samples and the geoelectric results revealed (in the last case see, for example, profile M4 in Fig. 7(b), which is a longitudinal profile through the site). In relation to point L5 for the shallowest interval, we observe that it also deviates from the respective tendency, probably due to the weather influence (i.e., rain). In the deepest interval the effect of moisture from the phreatic zone is evident, producing the lowest resistivity values, which are very similar among them and without a clear tendency. In the case of L4 (for the deepest interval) the chemical analyses also revealed high concentrations of hydrocarbon, so it cannot be determined from this kind of analysis if the low value is due to hydrocarbon or to moisture.

The previous analysis suggests that it is possible to establish a quantitative relation between resistivity and contaminant concentration for the three shallower intervals but not for the deepest. Nevertheless, complex resistivity contours occur in the 0.0–0.5 m depth interval, with noticeable fluctuations and low values along the profiles. This can be attributed to a significant weather influence. Then, it is not possible for this interval to simply and univocally determine if a given resistiv-

TABLE 3
Second series of analyses of PTH (EPA 418.1)

| Depth (m) | Q1 (mg/kg) | Q2 (mg/kg) | Q3 (mg/kg) | Q4 (mg/kg) |
|---|---|---|---|---|
| 0.0–0.5 | 0.6 | 1373.0 | 6204.0 | 2.2 |
| 0.5–1.0 | 0.6 | 1324.0 | 5148.0 | 230.0 |
| 1.0–1.5 | 0.5 | 1503.0 | 8119.0 | 156.0 |
| 1.5–2.0 | 0.7 | 6.3 | 5357.0 | 5.1 |

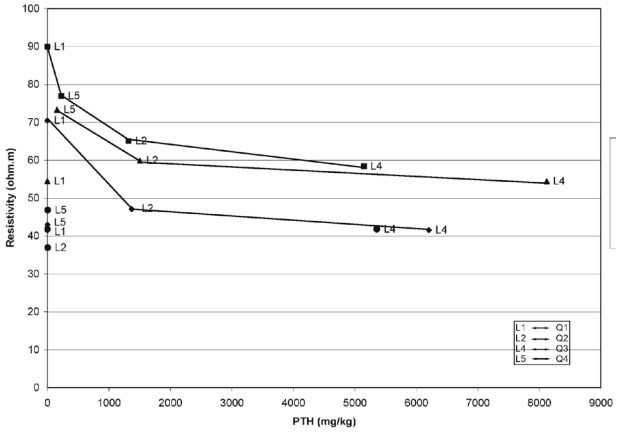


FIGURE 5
Average resistivity as a function of the level of contamination measured. The values belonging to each depth interval (0.0–0.5 m, 0.5–1.0 m, 1.0–1.5 m and 1.5–2.0 m) were jointed by means of a line.

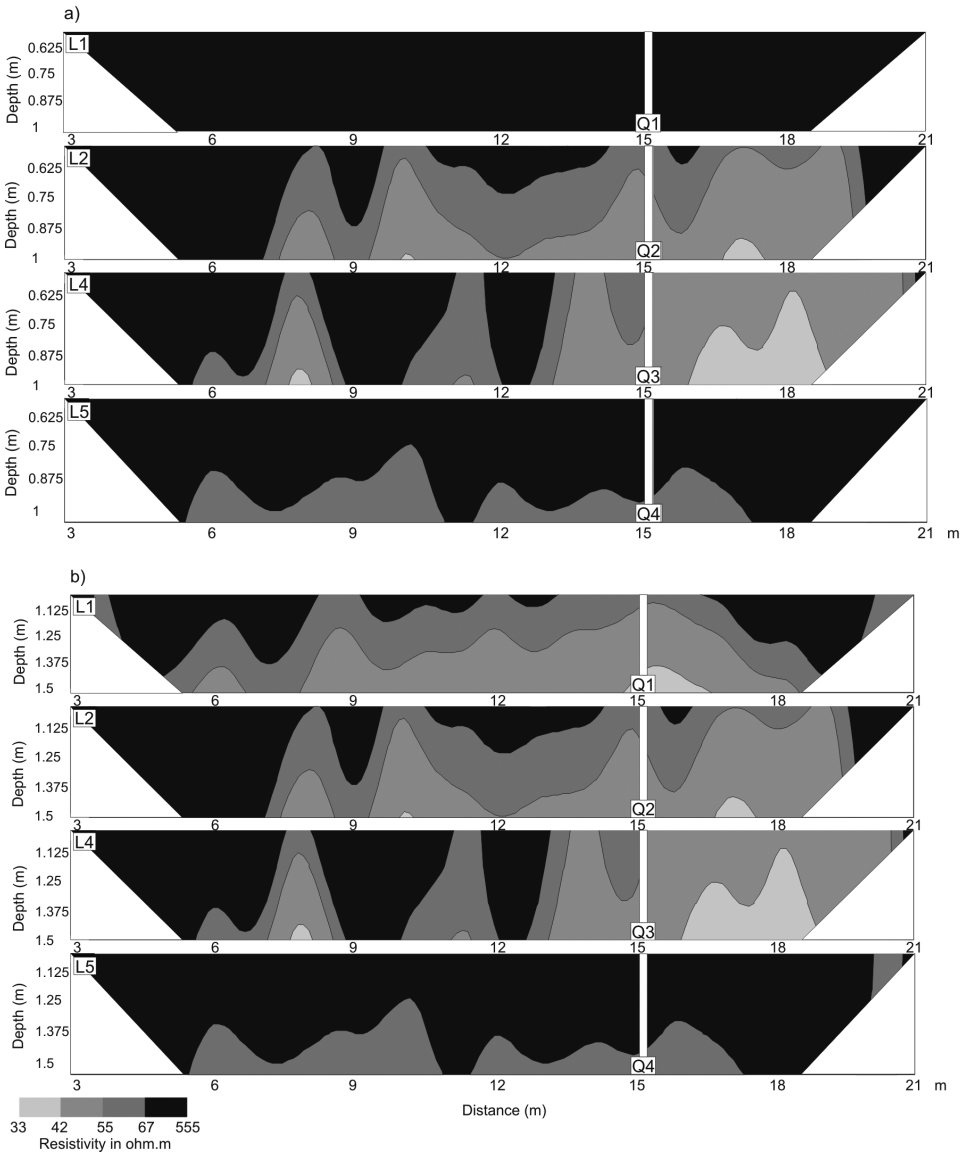


FIGURE 6
Resistivity profiles for lines L1, L2, L4 and L5. A colour was assigned to every resistivity interval 33–42 ohm.m, 42–55 ohm.m, 55–67 ohm.m and 67–555 ohm.m, in each of the depth intervals a) 0.5–1.0 m and b) 1.0–1.5 m. The second series of monitoring wells are indicated with Q#.

ity value is due to contaminant or to water. Therefore, we limit the analysis to the two intermediate-depth intervals, i.e., 0.5–1.0 m and 1.0–1.5 m, for which a minor influence of water occurs. Taking into account the local legal limit (1000 mg/kg) and the data distributions in Fig. 5 we define the following resistivity ranges for the analysis: 1) above 67 ohm.m, water influence is negligible and hydrocarbon concentrations are below the legal limit and 2) in the range 55–67 ohm.m, water influence is minor and hydrocarbon concentrations are above the allowed. Up to this point it is not clear if values less than 55 ohm.m are due to high concentrations of contaminant or to the influence of the phreatic zone.

In Fig. 6 we have horizontally divided profiles L1, L2, L4 and L5, considering the two intermediate depth intervals (0.5–1.0 m and 1.0–1.5 m, Fig. 6(a,b) respectively). We have used the aforementioned resistivity ranges for the colour scale (more precisely, the lower resistivity range has been subdivided into two). The resistivity intervals are the following: 33–42 ohm.m, 42–55 ohm.m, 55–67 ohm.m, 67–555 ohm.m. The lowest limit, 33 ohm.m, corresponds to the absolute minimum in the profiles. This value is similar to those measured for the phreatic zone: 30–41 ohm.m. To obtain the last interval we have considered the profiles in Fig. 4 and averaged the resistivity along each of them and below the top level of the phreatic zone (2.5 m, as indicated by the chemical analyses). Then, the range 33–42 ohm.m is representative of the sectors that could be more influenced by the phreatic zone. The intermediate range, 42–55 ohm.m, corresponds to sectors with less or even no significant influence of it. Finally, for the other two intervals the effects of water are assumed negligible. The upper limit, 555 ohm.m, corresponds to

TABLE 4
Semi-quantitative relation between resistivity and contamination level

| Resistivity (ohm.m) | Contamination level in the sector |
|---|---|
| <55 | Contaminated or not, depending on the shape of the anomaly |
| 55–67 | Contaminated |
| >67 | Not contaminated or below the legal limit |

the maximum resistivity measured.

When we analyse profiles L1, L2, L4 and L5 in Fig. 6(a), for the depth interval 0.5–1.0 m, it can be observed that the resistivity values are above 67 ohm.m, below the contamination limit. This result agrees with the chemical analyses performed at the Q# wells. Although in the most shallow portion of profile L5 there is a narrow and approximately horizontal fringe with values in the range 55–67 ohm.m, we consider that it is simply due to a transition between this interval and the weathered layer. On the contrary, in the L2 and L4 profiles sectors can be observed with resistivities between 42–67 ohm.m; they present shapes that are clearly different to the previous, vertically crossing the interval. Wells that presented the highest levels of contamination precisely locate within these sectors, so a relation between these anomalous sectors and the contaminant seems evident.

In relation to the depth interval 1.0–1.5 m (Fig. 6b), profiles L1 and L5 also present sectors with resistivities less than 67 ohm.m. Nevertheless, their approximately horizontal shapes and the lack of continuity towards the immediate superior interval indicate a transition between these sectors and the phreatic zone, rather than the existence of contaminant. From a comparison of both profiles, it can be checked that in L1 the phreatic zone is shallower. On the contrary, in profiles L2 and L4 sectors can be observed with resistivities below 67 ohm.m, approximately vertical shapes and continuity towards the immediate upper stratum, which seems to indicate the contaminant flux. Note that, in general, it is not only the resistivity of the anomaly but also its shape that allow us to characterize it. As a synthesis, we can establish a semi-quantitative relation between resistivity and contamination level in the sector, which is shown in Table 4.

## Remediation

The explained procedures allowed us to delimit the affected areas. These results were useful to determine the amount of soil to be treated in order to analyse the different remediation methods and choose an effective one.

Land farming is an above-ground remediation technology for soils that reduces concentrations of petroleum constituents through biodegradation. In Argentina, biological treatments like this are prohibited by federal laws in areas located near roads, so these kinds of methods were dismissed.

The stabilization/solidification (*in-situ*) technique (Khan *et al.* 2004) has the objective of including the contaminant phase within a solid isolated matrix. In this way, any possible excess of liquid is eliminated and the risk of lixiviation is reduced. With the solidification we obtain, by means of the addition of materials such as Portland cement, a monolithic solid with the contaminant trapped or being part of a solid matrix. We chose this technique because the amount of contaminated soil was so large that its removal for incineration and the subsequent replacement by new soil, would have been extremely expensive.

Some relevant topics during the design of the stabilization process were to determine the optimum proportion in the mixture of soil and Portland cement, to determine the time to complete the whole procedure and to analyse which will be the volume of the solidified product and the isolating box. Remediation activities were performed from 7 August to 31 October 2006. These activities included: a) the construction of an isolating box, b) the stabilization and solidification of the contaminated material, c) the final covering and isolating of the treated material and d) the designing and beginning of a post-remediation monitoring plan. The lateral isolating screen (which is represented by a solid line in Fig. 3b) had a width of 0.6 m up to a depth of 2.5 m. The bottom screen had a thickness 0.3 m and the top screen 0.1 m, which was deployed in order to block the infiltration of shallow water. As a preventive action the size of the insulating screen slightly exceeded the zone indicated by the geophysical studies, also extending it towards the areas that presented less vegetation on the surface. The mixture used to build the isolating screen presents the following composition: 64.5% unpolluted soil, 5.2% Portland cement and 30.3% water.

The contaminated soil was mixed with Portland cement and water. In this case, the mixture contains: 62.7% soil, 6.9% Portland cement and 30.4% water. This kind of mixture was used to stabilize the soil with high contents of hydrocarbons (more than 1000 mg/kg). Once solidificated, this material was relocated within the box and then isolated through the aforementioned top screen.

## Post-remediation monitoring

*Chemical analyses*

After the remediation, six inspection wells were drilled up to a depth of 3 m, where the phreatic zone and the presence of NAPL were monitored. Water monitoring has been performed from them every six months, with no contamination found after five periods.

*Geophysical survey*

The area prospected by the EMI method after remediation was larger than the previously prospected area, as seen in Fig. 2. A slice view of the inverted EMI data at 1 m depth is shown as an example in Fig. 3(a). An anomalous zone whose location agrees with the remedied area can be clearly observed in the figure.

The location of the geoelectrical dipole-dipole profiles performed after the remediation are shown in Fig. 2 and the inversion results of them are shown in Fig. 7. Profiles M1, M2 and M3 (Fig. 7a) were perpendicular to the road, whereas profiles M4 and M5 (Fig. 7b) were parallel to it. M1, M3 and M4 were

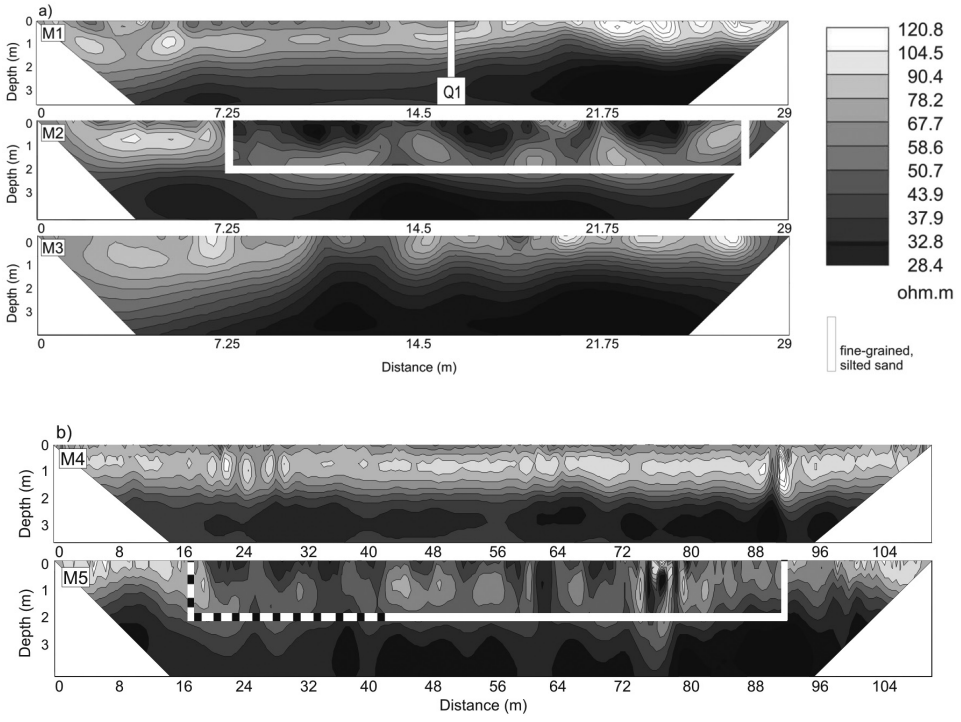


FIGURE 7
Images of the resistivity after the remediation. a) Lines M1, M2 and M3 perpendicular to the road. They were respectively located at 13.0 m, 61.5 m and 95.0 m. A monitoring well is also indicated in the M1 profile. b) Lines M4 and M5 parallel to the road at 6.5 and 18 m. With a white solid line we delimited the remediate zone (M2 and M5 profiles).

located outside the zone of remediation; M2 and M5 were carried out across it (the area has been delimited by solid lines in the figures). From profile M4 it can be checked that the phreatic zone is shallower towards the beginning of the profiles (due to the small slope in the ground). It can be observed that the box for the remediation produced a conductive anomaly over a more resistive layer. The anomaly extends from 7–27 m in the perpendicular direction, and from 16–94 m along the road. The last characteristic is mainly due to the cement component in the box, whereas in the upper layer the soil increased its electrical conductivity due to the weather effects. When we compare profiles L1 and M1, which were acquired at coincident locations but with a 7 months interval, we note different resistivity distributions up to 1 m depth, which is probably a consequence of different precipitation histories for both profiles.

From these figures we can see that the anomalous zone did not extend outside the box. This fact jointly with the monitoring well results, confirmed that the contaminant is encapsulated. Then, we can conclude that the remediation has been successful.

## CONCLUSIONS

In the present article, we jointly use EMI, geoelectrical and traditional chemical methods to characterize a zone where a hydrocarbon leakage had occurred. The joint implementation allowed us to delimit the affected portions of soil, from which we could select an adequate remediation procedure. Although each one of these methods, when used separately, does not provide the desired rapid and precise identification of the contaminated zones, they proved effective when jointly implemented.

The success of the remediation was confirmed by the monitoring performed afterwards, which showed that no permanent environmental damage was produced. Samples from nearby unaffected zones where also extracted and no contamination was found there.

A number of factors caused that the impacted zone remained laterally constrained and shallow, so neither the cultivated area nor the aquifer were affected: 1) part of the hydrocarbon lying on the surface was removed immediately after the accident, reducing the quantity of hydrocarbon that could percolate, 2) due to the surface slope, contaminant was mostly spread in a longitudinal direction (parallel to the road), covering a relatively large area. In this way the vertical penetration was reduced, 3) the major shallow draining was towards the west, so the cultivated area was not affected and 4) biodegradation also contributed to the reduction of the spill as a prolonged time passed between the time of the accident and the remediation.

From the results of this work, it can be deduced that an efficient strategy to investigate a hydrocarbon contaminated soil can be:

**1** Locate anomalous electrical areas through a rapid EMI prospecting.
**2** From these results select a number of representative locations to perform geoelectrical profiles. Delimit geoelectrical anomalies and compare them with the EMI ones. Validate and precise the EMI results.
**3** Drill a reduced number of wells in selected zones and measure the pollution in them.
**4** Correlate the geophysical and chemical results in order to select the anomalies probably due to the contaminant.

Perform additional chemical analyses if necessary.

A rapid and precise localization of the possible contaminated sectors allows a more efficient distribution of the wells, with a consequent reduction in costs and time. Once the contaminated volumes of the soil have been delimited through this procedure, an adequate methodology of remediation can be established.

## ACKNOWLEDGEMENTS

This work was partially supported by CONICET (National Council of Scientific and Technological Research), ANPCyT (Agency of Scientific and Technological Promotion), Facultad de Ingeniería, Universidad Austral, Facultad de Ciencias Empresariales and Universidad Abierta Interamericana and La Segunda Insurance Co., Argentina.

## REFERENCES

Abdel Aal G.Z., Atekwana E.A., Slater L.D. and Atekwana E.A. 2004. Effects of microbial processes on electrolytic and interfacial electrical properties of unconsolidated sediments. *Geophysics Research Letters* **31**, L12505. doi:10.1029/2004GL020030

Atekwana E.A., Sauck W.A. and Werkema D.D. 2000. Investigations of geoelectrical signatures at a hydrocarbon contaminated site. *Journal of Applied Geophysics* **44**, 167–180.

Bongiovanni V., Bonomo N., de la Vega M., Martino L. and Osella A. 2008. Rapid evaluation of multifrequency EMI data to characterize buried structures at a historical Jesuit Mission in Argentina. *Journal of Applied Geophysics* **64**, 37–46.

EPA (Environmental Protection Agency) 1983. *Method 418.1, Total Recoverable Petroleum Hydrocarbons by Infrared Spectroscopy*. Methods for the Analysis of Water and Wastes, Washington DC.

Farquharson C. 2000. *Background for Program EM1DFM, 1D Modelling and Inversion Code for Frequency Domain Measurements*. University of British Columbia, Geophysical Inversion Facility (UBC-GIF).

Frohlich R.K., Barosh P.J. and Boving T. 2008. Investigating changes of electrical characteristics of the saturated zone affected by hazardous organic waste. *Journal of Applied Geophysics* **64**, 25–36.

Khan F. I., Husain T. and Hejazi R. 2004. An overview and analysis of site remediation technologies. *Journal of Environmental Management* **71**, 95–122.

Oldenburg D.W. and Li Y. 1994. Inversion of induced polarization data. *Geophysics* **59**, 1327–1341.

Oldenburg D.W., McGillivary P.R. and Ellis R.G. 1993. Generalized subspace method for large scale inverse problems. *Geophysical Journal International* **114**, 12–20.

Osella A., de la Vega M. and Lascano E. 2002. Characterization of a contaminant plume due to a hydrocarbon spill using geoelectrical methods. *Journal of Environmental and Engineering Geophysics* **7**, 78–87.

Reynolds J.M. 1997. *An Introduction to Applied and Environmental Geophysics*. John Wiley & Sons.

Sauck W. 2000. A model for the resistivity structure of LNAPL plumes and their environs in sandy sediments. *Journal of Applied Geophysics* **44**, 151–165

Sauck W., Atekwana E.A. and Bermejo J.L. 1998. Characterization of a newly discovered LNAPL plume at Wurtsmith AFB, Oscoda. 11th Annual Meeting EEGS, Chicago, Illinois, pp. 399–408.

Shevnin V., Delgado Rodríguez O.D., Mousatov A., Flores Hernández D., Zegarra Martínez H. and Ryjov A. 2006. Estimation of soil petrophysical parameters from resistivity data: Application to oil-contaminated site characterization. *Geofísica Internacional* **45**, 179–193.

UBC-GIF 2000. *DCIP2D. Forward Modelling and Inversion of DC Resistivity and Induced Polarization Data over 2D Structures*. University of British Columbia, Geophysical Inversion Facility.

de la Vega M., Osella A. and Lascano E. 2003. Joint inversion of Wenner and dipole–dipole data to study a gasoline-contaminated soil. *Journal of Applied Geophysics* **54**, 97–109.

Won I.J., Keiswetter D.A., Fields G.R.A. and Sutto L. 1996. GEM-2: A new multifrequency electromagnetic sensor. *Journal of Environmental and Engineering Geophysics* **1**, 129–137.